Multimodal molecular imaging of atherosclerosis: Nanoparticles functionalized with scFv fragments of an anti-αIIbβ3 antibody

Mélusine Larivière, Cyril Samuel Lorenzato, Laurent Adumeau, Samuel Bonnet, Audrey Hemadou, Marie-Josée Jacobin-Valat, Abdelmajid Noubhani, Xavier Santarelli, Laetitia Minder, Carmelo Di Primo, et al.

Multimodal molecular imaging of atherosclerosis: Nanoparticles functionalized with scFv fragments of an anti-αIIbβ3 antibody☆

Mélusine Larivière, PhD[a,1], Cyril Samuel Lorenzato, PhD[a,*,1], Laurent Adumeau, PhD[b], Samuel Bonnet, MSc[a], Audrey Hémadou, PhD[a], Marie Josée Jacobin Valat, PhD[a], Abdelmajid Noubhani, PhD[c], Xavier Santarelli, PhD[c], Laetitia Minder, MSc[d,e], Carmelo Di Primo, PhD[d,f], Stéphane Sanchez, MSc[a], Stéphane Mornet, PhD[b], Jeanny Laroche Traineau, PhD[a,2], Gisèle Clofent Sanchez, PhD[a,2]

[a]*Centre de Résonance Magnétiques des Systèmes Biologiques, Bordeaux, France.*
[b]*CNRS, Univ. Bordeaux, Bordeaux INP, Pessac, France.*
[c]*Bordeaux INP, Pessac, France.*
[d]*Université de Bordeaux, Pessac, France.*
[e]*Institut Bergonié, SIRIC BRIO, Bordeaux, France.*
[f]*Université de Bordeaux, Laboratoire ARNA, Bordeaux, France.*

Abstract

Due to the wealth of actors involved in the development of atherosclerosis, molecular imaging based on the targeting of specific markers would substantiate the diagnosis of life threatening atheroma plaques. To this end, TEG4 antibody is a promising candidate targeting the activated platelets (integrin αIIbβ3) highly represented within the plaque. In this study, scFv antibody fragments were used to functionalize multimodal imaging nanoparticles. This grafting was performed in a regio selective way to preserve TEG4 activity and the avidity of the nanoparticles was studied with respect to the number of grafted antibodies. Subsequently, taking advantage of the nanoparticle bimodality, both near infrared fluorescence and magnetic resonance imaging of the atheroma plaque were performed in the ApoE$^{-/-}$ mouse model. Here we describe the design of the targeted nanoparticles, and a quantification method for their detection in mice, both *ex vivo* and *in vivo*, highlighting their value as a potential diagnosis agent.

Key words: Atherosclerosis; Bimodal imaging; scFv antibody fragments; Directed conjugation; SPIO; Near infrared fluorescence (NIRF)

Atherosclerosis is one of the most important health conditions worldwide, from which originate the majority of acute cardio vascular events. Official statistics state that 17.5 million people die each year from cardio vascular diseases (CVD), 80% of all CVD deaths being due to heart attacks and strokes.[1]

Abbreviations: scFv, single chain variable fragment; ApoB, Apolipoprotein B; ApoE$^{-/-}$ mouse, Apolipoprotein E knockout mouse; SPR, surface plasmon resonance; IHC, immunohistochemistry; NIRF, near infrared fluorescence; MRI, magnetic resonance imaging; (V)USPIO, (Versatile) Ultrasmall superparamagnetic iron oxide; LDL, low density lipoproteins; IMAC, Immobilized metal affinity chromatography; SDS PAGE, sodium dodecyl sulfate polyacrylamide gel electrophoresis

Authors contributions:

Sources of funding

*Corresponding author at: Centre de Résonance Magnétiques des Systèmes Biologiques (CRMSB), Bordeaux Cedex, France.

E-mail addresses: melusinelariviere@gmail.com, (M. Larivière), cyril.lorenzato@u bordeaux.fr, cyril.lorenzato@gmail.com, (C.S. Lorenzato), laurent.adumeau@cbni.ucd.ie, (L. Adumeau), samuel.bonnet@rmsb.u bordeaux.fr, (S. Bonnet), audrey.hemadou@orange.fr, (A. Hémadou), marie josee.jacobin@rmsb.u bordeaux2.fr, (M. J. Jacobin Valat), noubhani@bordeaux inp.fr, (A. Noubhani), xavier.santarelli@bordeaux inp.fr, (X. Santarelli) , l.minder@iecb.u bordeaux.fr, (L. Minder), carmelo.diprimo@inserm.fr, (C. Di Primo), stephane.sanchez@rmsb.u bordeaux.fr, (S. Sanchez), stephane.mornet@icmcb.cnrs.fr, (S. Mornet), jeanny.laroche@rmsb.u bordeaux.fr, (J. Laroche Traineau), gisele.clofent sanchez@rmsb.u bordeaux.fr. (G. Clofent Sanchez).

[1] These authors contributed equally, ML and CSL are first coauthors

[2] These authors contributed equally, JLT and GCS are senior coauthors

Atherosclerosis gradually develops for fifty or more years throughout the life of an individual under the influence of multiple lifestyle, environmental, and genetic factors. It leads to chronic ischemic complications or acute lethal events like myocardial infarction or stroke.

The pathogenesis of atherosclerosis depends on (1) an increased level of circulating atherogenic lipoproteins,[2] and (2) local immuno inflammatory factors.[3,4]

Primary intimal lesions develop under the influence of local hemodynamic stress, usually at the branching points of major arteries. There, low density lipoproteins (LDLs) accumulate on the endothelial surface, forming structures called fatty streaks, which in turn trigger the recruitment, activation, and differentiation of monocytes into macrophages.[5,6] Reactive oxygen species resulting from the inflammatory environment react with LDL to form oxidized LDL (oxLDL): when oxidized, ApoB binds scavenger receptors of macrophages, thus leading to the formation of LDL laden macrophages called foam cells.[7] Activated endothelial cells and platelets express adhesion molecules such as P selectin and intracellular adhesion molecule 1 (ICAM1) mediating the interaction with leukocytes and their subendothelial accumulation. Platelets bear glycoproteins GPIbα responsible for their adhesion to the vessel wall, GPαIIbβ3 responsible for their aggregation and thrombus formation and GPIV (CD36) which binds oxLDL,[8,9] contributing to the development of the plaque.[10] In a recent study, we underlined the presence of platelets not only in thrombi and intraplaque hemorrhage, as expected, but also in atheroma burden, around necrotic areas and neovessels, shedding light on the rationale for targeting platelets within atherosclerotic lesions.[11]

Indeed, atheroma burden assessment in the clinics nowadays relies on a combination of clinical signs, biological factors, and imaging. The methods currently used to locate the lesions are mostly invasive intravascular imaging. On the other hand, non invasive imaging only detects local stenosis. Current development efforts are thus directed towards molecular imaging, able to assess not only the anatomical structure of the plaque, but also its activity: inflammation state, fibrosis, calcification, *etc.*[12]

Taking advantage of the rich plaque composition, previous works have studied the feasibility of addressing various kinds of nanocarriers to the plaque, in order to deliver either therapeutic factors or imaging contrast agents. Mostly, this targeting was achieved either passively, using the outermost layer of coating of the injected objects,[13,14] or with surface conjugated peptides.[15,16]

In this regard, TEG4, a monoclonal human antibody targeting integrin αIIbβ3, selected by phage display technology,[17] has previously been used as a full IgG targeting agent for molecular imaging. We first demonstrated that TEG4 targets platelets in atheroma lesions both *in vitro* and *ex vivo*. We also showed that iron oxide based nanoparticles (VUSPIO for Versatile Ultra Small SuperParamagnetic Iron Oxide[18]) functionalized with TEG4 were still able to bind platelets both *in vitro* and *ex vivo*, and could be detected by transmission electron microscopy and magnetic resonance imaging (MRI).[11]

In this study, we investigated the effect of multivalent, site specific grafting of single chain variable fragment (scFv) antibody fragments of the platelet reactive TEG4 antibody on the reactivity of functionalized VUSPIO nanoparticles. Compared to full IgGs (150 kDa), scFv fragments (35 kDa) present a reduced size, which makes them more suitable for functionalizing relatively small nanoparticles (90 nm), and allows increasing the particle valence, *via* the conjugation of several fragments. In this regard, to better control the antibody to probe conjugation ratio and the fragment orientation, this scFv was engineered to present two terminal cysteines that allowed for site directed grafting to maleimide residues on the surface of the nanoparticle.[19] Indeed, usual conjugation strategies involve the reaction of amine side chains of the antibodies, which may be a good strategy for full IgG but presents the risk to degrade the binding sites of smaller antibody fragments and impede their reactivity. Avidity and reactivity of the functionalized nano object were assessed *in vitro* by surface plasmon resonance (SPR) on purified integrin αIIbβ3 and immunohistochemistry (IHC) on fixed atheromatous tissue, and confirmed the expected benefit of multifunctionalization.

In addition, fluorochromes were attached to the surface of the VUSPIO to allow for a multimodal near infrared fluorescence (NIRF) MRI detection. The potential for bimodal imaging of the lesions by NIRF and MRI measurements was thus explored by *ex vivo* injections in aortas of $ApoE^{-/-}$ model mice, which were highly promising, showing potential for the object as a biocompatible, atheroma specific diagnosis agent. Upon *in vivo* injection in the same model, efficient targeting with functionalized nanoparticle could be demonstrated 20 min after injection, and up to 24 h.

Nowadays, atherosclerosis imaging remains a challenge, although several teams have described methods for MRI detection of atheroma with passive[20–22] or targeted[23–25] contrast agents. In addition to these studies, which allowed for preclinical advances in MR based atherosclerosis imaging, we here propose a robust way to overcome the limitations exhibited by classical image based interpretation, and to assess the presence of the lesions in a statistically significant and reproducible manner. Our results were analyzed thanks to a custom made *in silico* method, allowing for a semi quantitative evaluation of the binding.

Methods

Animal models

Animal studies were approved under the No. 50120192 A by the Animal Care and Use Committee of Bordeaux, France. Adult male New Zealand rabbits (NZW) were obtained from Charles Rivers Laboratories, fed a fat atherogenic diet including 0.3% cholesterol for 8 months and subjected to surgeries to trigger the formation of complex plaques with intramural thrombi. Briefly, rabbits were subjected to two surgeries: (1) the mechanical removal of endothelial cells of the thoracic and abdominal aortic areas carried out by pulling back a Fogarty probe 4F along the endothelium. Then, two months later, (2) an angioplasty under radioscopic control with the aid of a balloon (20 mm long and 4.5 mm in diameter) inflated every 2 cm from the region of renal arteries to iliac bifurcation. Healthy rabbits from the same strain and provider were used as control.

ApoE$^{-/-}$ mice were obtained from Charles River Laboratories and fed a high cholesterol diet (0.15% cholesterol, Avogadro Western diet, Safe, Augy, France) for 21 weeks to allow for the development of atherosclerotic lesions. The atheroma plaque development in individual mice was followed up by MRI (see infra). Wild type control C57BL6 mice were used as a negative control (Charles River Laboratories, St Germain sur l'Arbresle, France).

Site specific multivalent grafting onto VUSPIO nanoparticles

VUSPIO nanoparticles synthesis was performed as described by Mornet et al.[2,3] After near infrared emitting dye (DyLight™ 800 Maleimide, Thermo Scientific, Illkirch, France) labeling, the primary amine terminal groups were converted into maleimide functions to allow for scFv grafting. A heterobifunctional NHS PEG maleimide spacer arm was first grafted on the surface amines of the VUSPIO nanoparticle and then reacted with the "activated" scFv. A fixed quantity of VUSPIO particles was mixed with increasing quantities of scFv so as to obtain theoretical scFv to VUSPIO molar ratios of 4 (R4, N = 4), 8 (R8, N = 3), 16 (R16, N = 6) and 32 (R32, N = 6). Commercially available irrelevant IgG (Jackson Immunoresearch Laboratories, West Grove, PA, USA) were conjugated as described in Jacobin Valat et al[3] to produce a control VUSPIO IgG. A detailed protocol is available in Supporting Information.

Avidity measurement

Surface plasmon resonance (SPR) experiments on purified αIIbβ3 integrin (Enzyme Research Laboratories, Swansea, UK) were carried out with a Biacore T200 instrument using CM5 sensor chips (GE Healthcare Europe GmbH, Velizy Villacoublay, France) and HBS Ca running buffer (0.01 M HEPES, pH 7.4, 0.15 M NaCl, 2 mM $CaCl_2$, 0.005% v/v Surfactant P20). Calcium ions were added to allow the good folding of the αIIbβ3 integrin complex.

Purified αIIbβ3 was immobilized by amine coupling following the manufacturer's instructions (GE Healthcare, Aulnais /s bois, France). After 2200 resonance units (RU) of ligand were immobilized, the scFv and VUSPIO scFv samples were injected over the immobilized target at a flow rate of 20 μL/min for 2 min. VUSPIO scFv particles, differing in the number of ligands per nanoparticle (R8, R16, R32), were injected sequentially from the highest to the lowest dilution factor. The scFv alone was injected at 100 μg/mL as a control for its affinity to αIIbβ3.

Reactivity assessment

The reactivity of TEG4 2c scFv alone, and after grafting to the VUSPIO was confirmed by IHC on paraffin embedded sections of arterial tissue from atherosclerotic and healthy rabbits, ApoE$^{-/-}$ mice and human patients (see Supporting Information).

After the sections were deparaffinized, rehydrated, and heat mediated antigen retrieval was performed, VUSPIO 0 or VUSPIO TEG4 corresponding to R8, R16 and R32 ratios were applied to the slides, diluted to the same iron concentration so as to compare the avidity of the VUSPIO in each batch. TEG4 2c scFv alone was applied to the slides in concentrations matching the calculated scFv content in each VUSPIO dilution to compare their reactivity. Following overnight incubation, a secondary HRP conjugated antibody specific to 6His (Sigma Aldrich, St Quentin Fallavier, France; working dilutions 1:250) was applied to the sections. Finally, after staining was performed by adding the peroxidase substrate diaminobenzidine (DAB substrate kit, Eurobio/ABCys, Les Ulis, France), slides were counterstained in hematoxylin, dehydrated and mounted. Quantification was made using the IHC Profiler Open Source Plugin (https://journals.plos.org/plosone/article?id=10.1371/journal.pone.0096801).

Ex vivo imaging procedure

ApoE$^{-/-}$ mice fed a high fat diet or control C57BL/6 wild type mice were terminally anesthetized by inhalation of isoflurane (Belamont, Nicholas Piramal Limited, London, UK). The aorta was exposed and immediately washed by intra cardiac injection of PBS heparin (3 mL, 50 UI/mL; Sanofi Aventis, Vitry sur Seine, France), followed by PBS alone (10 mL). Then a solution of either multivalent VUSPIO TEG4, VUSPIO IgG or PBS was injected through the left ventricle and incubated for 20 min before rinsing with PBS. The heart and aorta were then removed and fixed in paraformaldehyde (PFA) 4% v/v (Eurobio, Les Ulis, France) for subsequent imaging.

Fluorescence images were acquired using the Fluobeam 800 imaging device (Fluoptics, Grenoble, France), using 200 and 1000 ms exposure times.

After embedding in agarose gel (0.8% w/v) in a tube, high resolution MR imaging was performed on a horizontal 7 T Biospec system (Bruker, Ettlingen, Germany). A 72 mm birdcage resonator was used for RF transmission and the Bruker quadrature Rat Brain coil was used for RF reception. T_2^* maps were calculated from a RF spoiled multi gradient echo (MGE) images (repetition time TR = 1000 ms, first echo time TE = 3.2 ms, ΔTE = 3.6 ms, number of echoes = 15, α = 30°, spatial resolution = $0.075^2 \times 0.25$ mm^3, NEx = 32, 12 slices).

In vivo imaging procedure

Animals were anesthetized with 2% isoflurane (Belamont, Nicholas Piramal Limited, London, UK) in air for all imaging procedures. For MRI acquisitions, the isoflurane rate was adjusted overtime in order to maintain the monitored respiration rate to 60 bpm.

After at least 5 months of diet, the atheroma plaque burden in individual mice was evaluated by MRI on a horizontal 4.7 T Biospec system (Bruker, Ettlingen, Germany). Abdominal aorta was imaged in order to confirm the presence of atheroma plaques.

In animals with detectable atherosclerosis, multivalent fluorescent VUSPIO TEG4 particles were injected in a quantity corresponding to 4 mg of iron per kg of body weight (4 mg.kg^{-1}). Mice were imaged by MRI and fluorescence imaging. Basal images before injection were acquired for each *in vivo* technique. Non injected and VUSPIO 0 injected mice served as controls. Images were acquired before, after 20 min and 24 h following the injection of nanoparticles. Comparison of MR

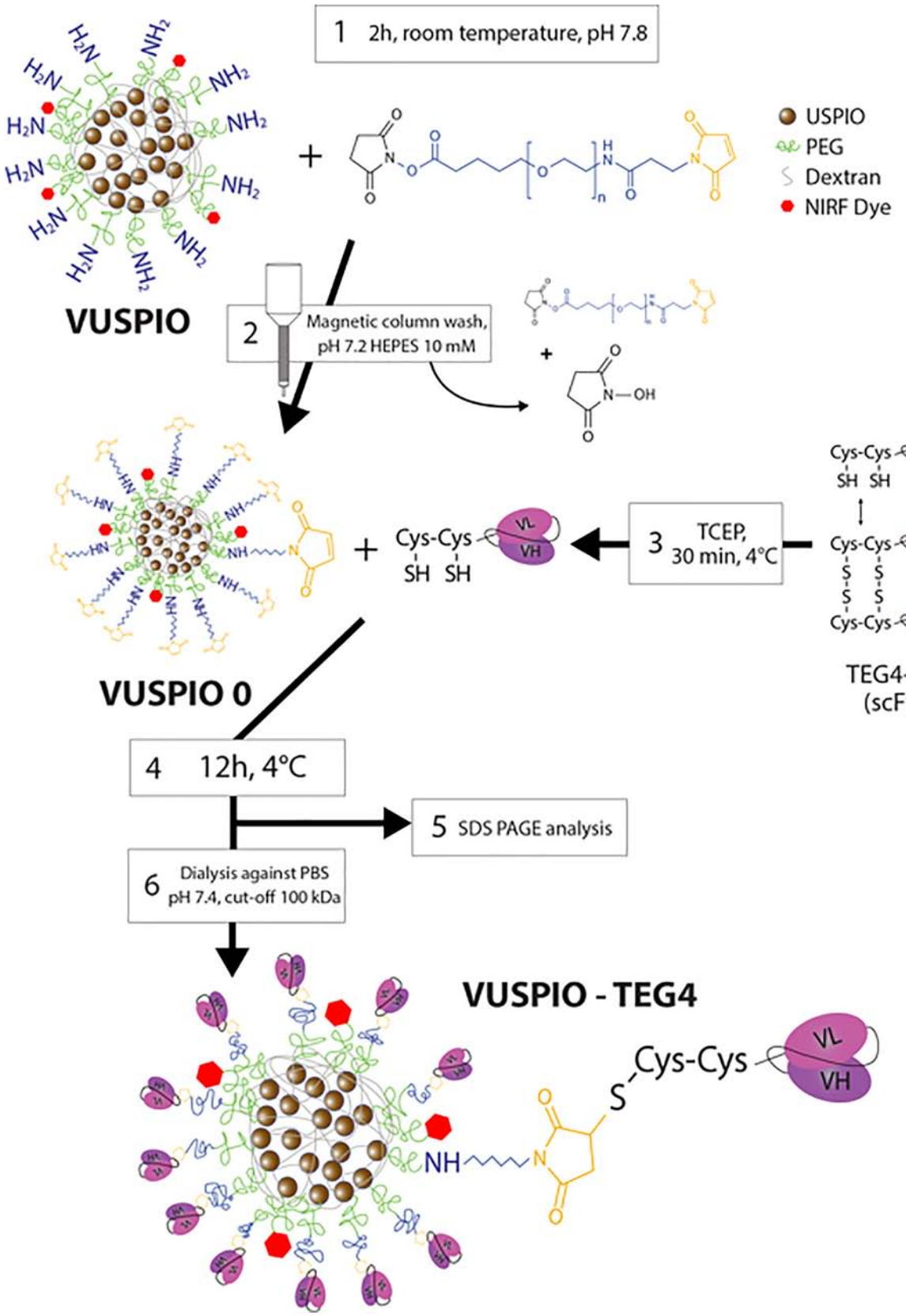

Figure 1. Schematic workflow for the conjugation process. 1: an excess NHS PEG mal is reacted onto the surface amines of the particle, 2: the VUSPIOs are washed on a magnetic column to remove the unreacted PEG and stop the reaction, 3: scFvs are activated by reduction with TCEP, 4: activated scFvs react with the surface maleimide of the VUSPIO for 12 h, 5: the grafting yield is determined by gel analysis before 6: the excess scFvs are cleaned by dialysis against PBS.

signal before and after injection was based on the estimation of R2* (= 1/T2*) for each voxel.

After the last image was acquired, the animals were humanely killed and dissected, while fluorescence imaging was performed at the Vivoptic facility in Bordeaux, using the Fluobeam imager (see supra). A blood sample was immediately retrieved from the cava vein and all remaining blood washed from the circulatory system and organs with a 3 mL PBS heparin (50 U/mL), followed by a 10 mL PBS intracardiac perfusion.

Results

Site specific multivalent grafting onto VUSPIO nanoparticles

Site specific conjugation was conducted *via* the two terminal cysteines on the scFv fragment and the maleimide residues on the surface of the VUSPIO nanoparticle[1] according to the workflow presented in Figure 1.

Avidity measurement

The avidity of the TEG4 2c scFv before and after grafting to the VUSPIO was assessed by surface plasmon resonance (SPR) sensing on purified αIIbβ3 integrin coated with around 2000 RU (2 ng/mm^2). This protein density was chosen to reflect endogenous αIIbβ3 receptor densities at the surface of activated platelets (1.7 ng/mm^2 considering a molecular weight of 250 kDa for αIIbβ3 and 50,000 αIIbβ3 per platelet with a diameter of 2 μm). scFv alone being monovalent, they should exhibit lower affinity (no avidity) compared to their bivalent, full IgG counterpart. However, their smaller size allowing for the grafting of several fragments, resulting multivalency should benefit to the global avidity of the nanoparticle.[6] To confirm this, each VUSPIO scFv sample was diluted according to its iron content, in order to assess the expected increase in avidity for each ratio (Supporting Information).

Dilutions of ratios R8, R16 and R32 were injected sequentially, from the highest to the lowest dilution factor, as shown in Figure 2, *A*. All three ratios exhibited a similar concentration dependence of the binding profile. The representative curves obtained for the 1/6 dilution, corresponding to a same order of magnitude of iron concentration (between 4.5 and 7.5 mM), are shown by Figure 2, *B*, together with the sensorgram corresponding to a 100 µg/mL concentration of free scFv prepared in solution. The SPR association curves of the multivalent VUSPIO scFv did not reach equilibrium and continued to show gradual increase during the 2 min association phase. The association/dissociation curves represent a quicker association and higher maximum bound analyte for the R32 compared to the R16, itself superior to the R8. The great influence of the avidity effect was clearly highlighted with the R32 batch, which showed a higher association rate compared to other batches, for the same order of magnitude of VUSPIO particles concentration. Additionally, R16 and R32 batches, although they were tested at similar scFv concentrations (7.8 and 12.8 μg/mL respectively), exhibited different behaviors. All three batches showed low to no dissociation compared to TEG4 2c scFv alone (Figure 2, *B*). Free scFv behaved quite differently from multivalent VUSPIO scFv batches with fast association and dissociation rates.

SPR sensing confirmed that the VUSPIO TEG4 binding avidity increased with the number of grafted scFv. The multivalence obtained thanks to an optimized grafting of scFv fragments on the VUSPIO nanoparticle can greatly increase the binding affinity of the monovalent TEG4 2c scFv. However, the resulting sensorgrams could not be fitted using a Langmuir binding model and an dissociation equilibrium constant could not be determined from these experiments because of multivalent interactions, *i.e.* different molecules of scFv on the same nanoparticle resulting in a pseudo irreversible binding (95% of the binding remaining after 7 min), a phenomenon previously described.[7–9]

Reactivity assessment

Immunohistochemistry experiments were conducted to assess, on pathological tissues, both the TEG4 2c reactivity after the grafting process and the benefit of multifunctionalization. Immunohistochemistry showed that VUSPIO scFv retained

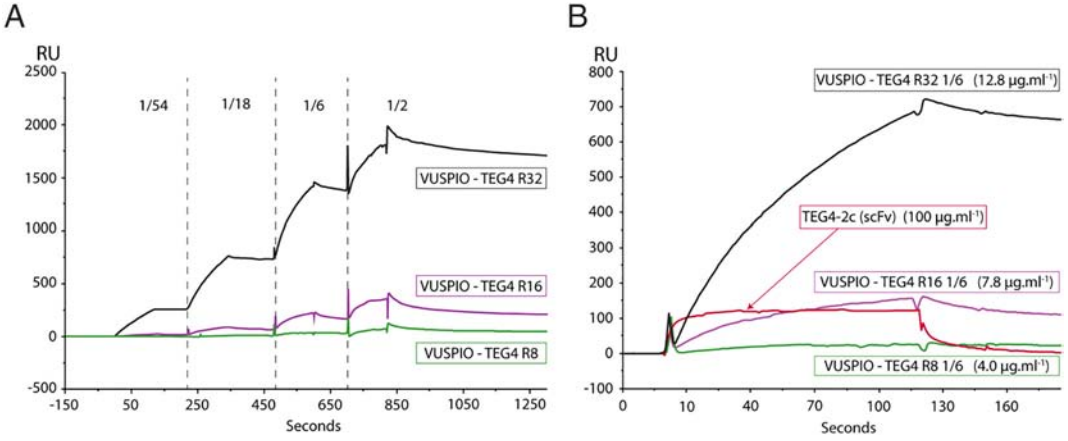

Figure 2. SPR analysis of the VUSPIO TEG4 particles. **(A)** Signal accumulation from each ratio measured at increasing iron concentration. **(B)** Comparison of the 4.5 7.5 mM iron concentration (1/6 dilution) for R8, R16 and R32 conjugation ratios. Data from sequential injections were extracted to construct this graph.

the reactivity of the unconjugated antibody. Indeed, upon incubation on atherosclerotic rabbit aorta slices, a specific staining of the areas of platelets accumulation in the atheroma plaque was observed (Figure 3). Oppositely, when incubated with bare VUSPIO particles or VUSPIO IgG control particles (previously shown in Jacobin Valat et al[11]), no staining could be observed. Moreover, when tested on healthy rabbit, VUSPIO TEG4 R32 did not accumulate in the healthy aorta. Similarly to the Biacore experiments, while the quantity of VUSPIO incubated on the slices remained constant, the staining intensity increased with the valence of the particles R8, R16, R32. The reactivity of TEG4 2c scFv in areas of platelet accumulation was also confirmed by immunofluorescence co staining on paraffin embedded sections of arterial tissue from mouse, rabbit and human (see Figure. S1, S2, S3 Supporting Information) to assess inter species cross reactivity, allowing for potential further translation to clinical studies.

Ex vivo imaging

Ex vivo experiments were performed in order to confirm the ability of the multivalent functionalized VUSPIO to access its target on a freshly resected aorta. Taking advantage of the bimodal imaging agent, both fluorescent and MR images of the aortas were acquired and compared. Figure 4, *A* shows ApoE$^{-/-}$ mice aortas either uninjected (Control) or injected with multivalent functionalized VUSPIO (TEG4 2c scFv or IgG) or VUSPIO 0. Each panel corresponds, from left to right, to the fluorescent image, the 7 T MR image and zoomed MR images. Dashed line boxes on fluorescence and MR images delineate the same locations on the aorta, which are zoomed for better visualization of the color scale in MR. On zoomed areas, dashed black arrows point to the normal vessel wall, black arrows to the atheroma plaque, and white arrow to the accumulation of the targeted contrast agent in atherosclerotic structures. Note that the

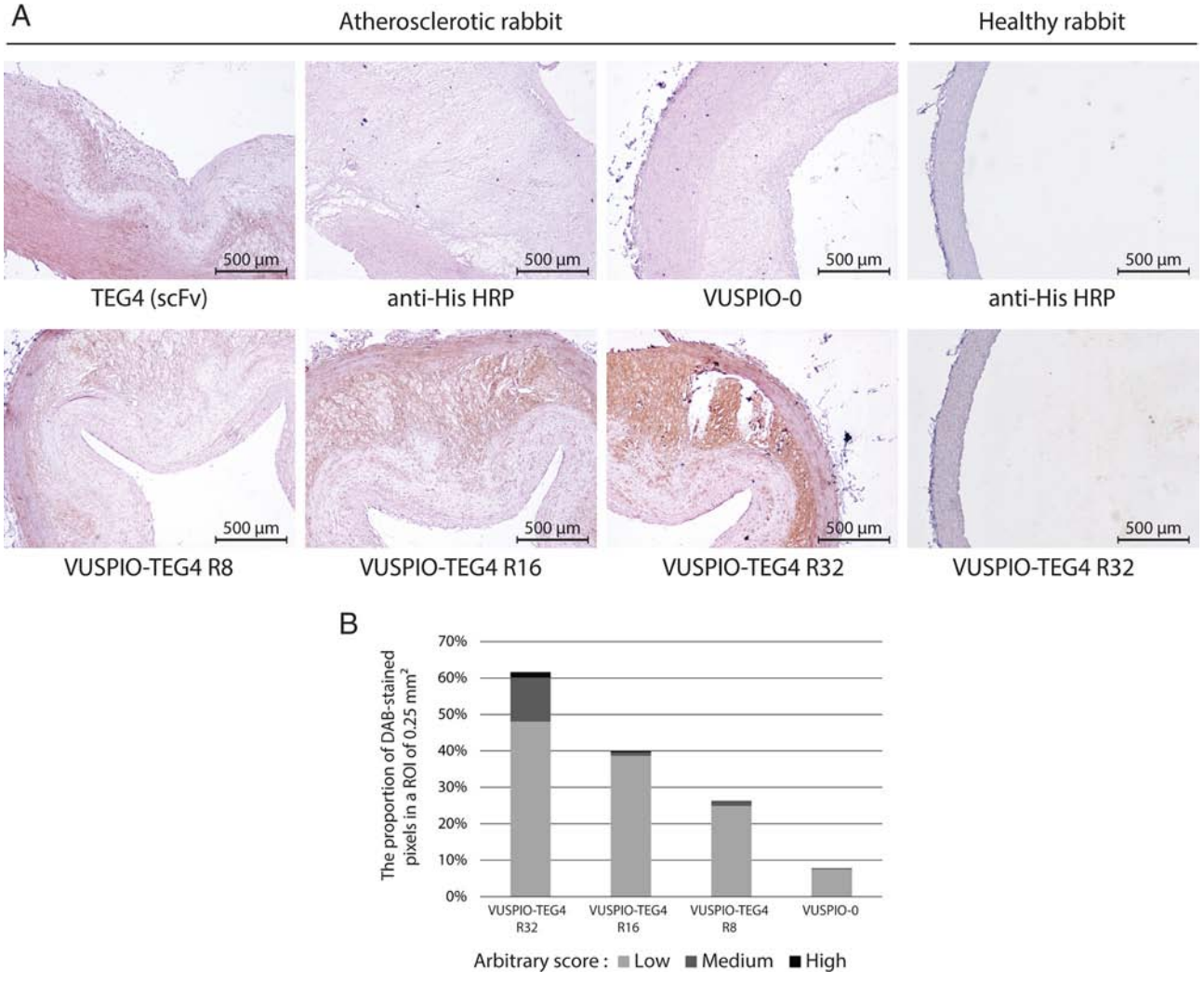

Figure 3. (A) Reactivity evaluation of VUSPIO TEG4. IHC analysis on atherosclerotic rabbit aorta of VUSPIO alone, 8 scFv to VUSPIO, 16 scFv to VUSPIO and 32 scFv to VUSPIO ratios. IHC analysis was also performed on sections of control rabbits with VUSPIO TEG4 R32. The unconjugated TEG4 2c scFv was used as a positive control. The secondary anti His HRP labeled antibody alone was used as a negative control. (B) Quantification was made using the IHC Profiler Open Source Plugin. (https://journals.plos.org/plosone/article?id 10.1371/journal.pone.0096801).

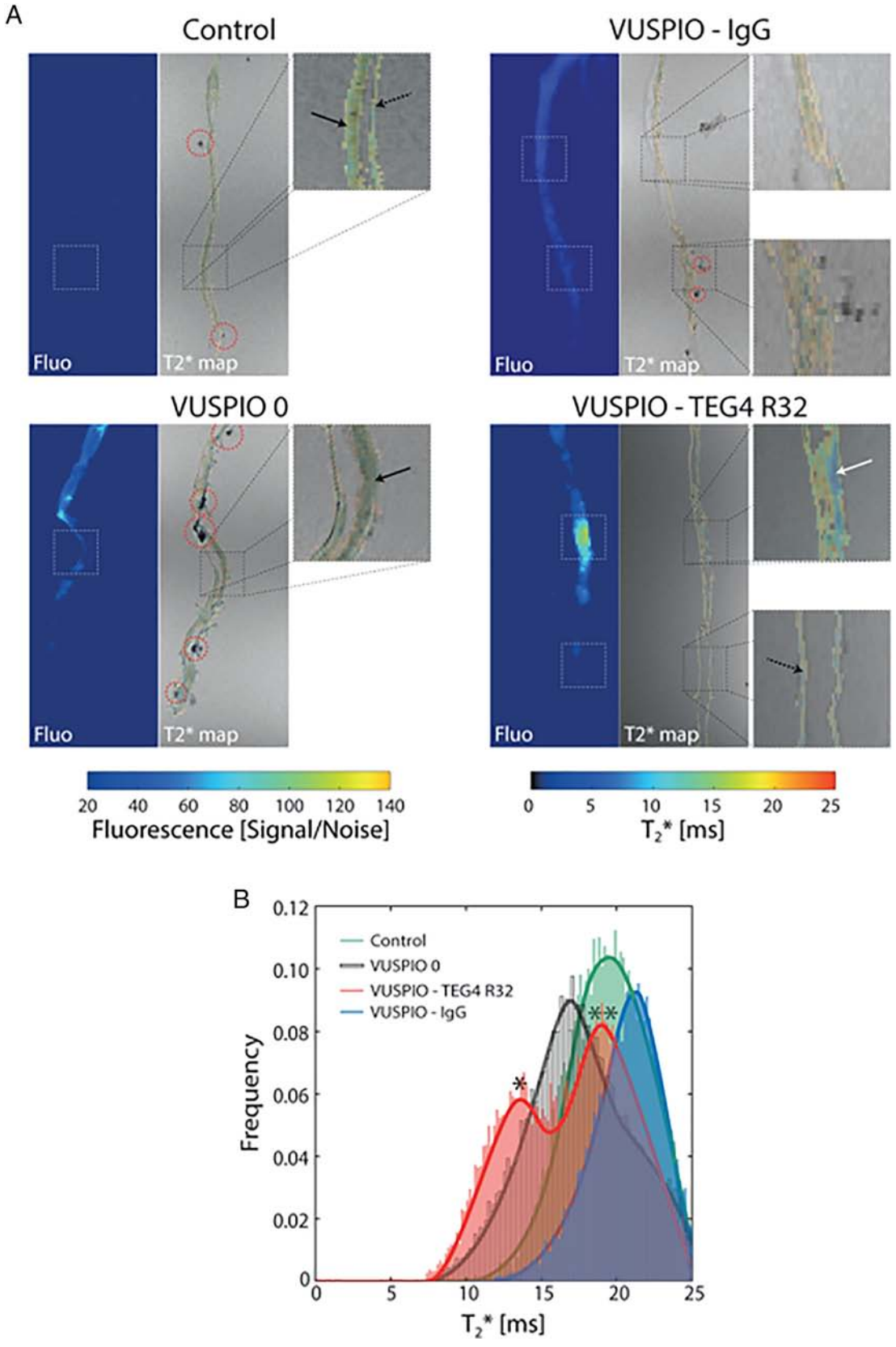

Figure 4. Fluorescent and MR images of atheromatous aorta. **(A)** Signal to noise ratio of fluorescence images (left) and their corresponding MRI magnitude images with segmented T_2* maps overlay (right) obtained from uninjected mice (control), after the injection of VUSPIO 0, VUSPIO IgG and VUSPIO TEG4 R32. **(B)** Distribution of T_2* originated from the segmented maps. Two peaks are clearly distinguishable after the injection of VUSPIO TEG4 R32 (*: mean $T_2^* \approx 13$ and **: mean $T_2^* \approx 19$).

dashed red circles point out air bubbles entrapped in the agarose gel.

No fluorescent signal was measured in the absence of injection, as demonstrated in the Control panel. Both VUSPIO IgG and VUSPIO 0 led to a low but detectable fluorescence signal that tended to decrease from the top to the bottom of the aorta, corresponding to the injection flow direction. Here it should be pointed out that localized but small fluorescence signals were sometimes observed (see VUSPIO 0 panel). These fluorescence signals were always found to colocalize with the presence of air bubbles (red dashed circles on MR images) entrapped into the aorta, as clearly evidenced by the correspond ing T_2* weighted MRI. On the contrary, intense fluorescence signals were measured in the VUSPIO TEG4 R32, which exactly corresponded to the plaque location (white arrow). The intimal thickening of the aorta, characteristic of an atherosclerotic plaque, was present in all mice (black arrows). Indeed, MR images resolution allowed for an anatomic discrimination of either the presence (plain arrows) or the absence (dashed arrows) of atheroma plaques (Figure 4, *A*), easily distinguished by the intimal thickening. However, these anatomically different areas presented quite similar segmented mean T_2^* values. This makes T2* maps suitable for the detection of VUSPIO nanoparticles, whose accumulation is known to induce a drop in the T2* signal. Differences in behavior were obtained between targeted and untargeted particles. Indeed, after VUSPIO TEG4 R32 injection,

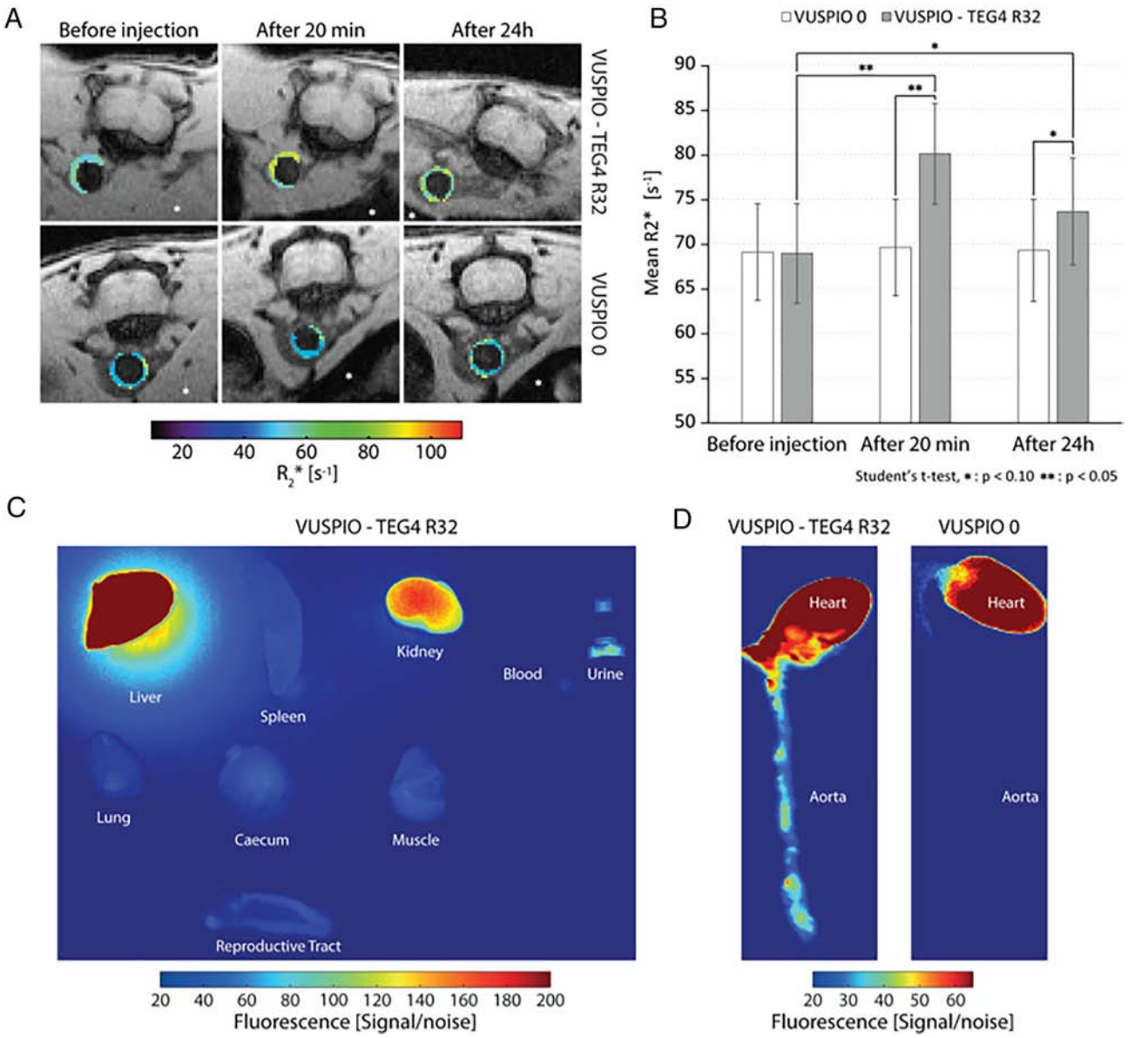

Figure 5. *In vivo* injection of VUSPIO TEG4 R32 compared to VUSPIO 0. **(A)** Segmented relaxation rate R_2* maps overlaid on their corresponding magnitude images obtained before and after the injections, *Indicates the liver. **(B)** Mean segmented R_2* values measured on at least six slices of N 6 mice for VUSPIO TEG4 R32 and N 3 mice for VUSPIO 0. **(C, D)** Nanoparticles fluorescence biodistribution imaging in dissected organs. Statistical analysis of the fluorescence distribution is shown in Table 1.

a local decrease of the T_2* colocalized with an intense fluorescence signal, which was not observed after VUSPIO 0 or VUSPIO IgG injection. Similarly, upon VUSPIO TEG4 R32 injection in age matched C57BL6 mice on a normal chow diet, no hyposignal was observed (Figure S6 in Supporting Informa tion). The decrease in the T_2* value was only measured where atheroma plaque was present, as shown in the zoomed image of VUSPIO TEG4 R32. Even if slightly dependent on the mice, as demonstrated in Figure 4, *B*, the control (T_2^* = 19.1 ± 3.2 ms), the VUSPIO 0 (20.9 ± 2.6 ms) and the VUSPIO IgG (18.9 ± 4.3 ms) segmented mean T_2^* values were homogenous. In contrast, thanks to the local accumulation of iron oxide nanoparticles, a sub T_2^* population (white arrow) with a clear decrease in the T_2* values (≈ 13 ms) was detected upon injection of VUSPIO TEG4 R32.

In vivo imaging

The ability of the multivalent VUSPIO TEG4 R32 to access its target *in vivo* was assessed by MRI by characterizing its accumulation 20 min and 24 h post injection. Afterwards, fluorescence based biodistribution studies and accumulation in lesions in the aorta were assessed *ex vivo*.

Figure 5, *A* shows the R_2* maps measured at the plaque level in ApoE$^{-/-}$ mice injected with either VUSPIO TEG4 R32 or VUSPIO 0 at 4 mg kg^{-1} of iron. Twenty minutes after the injection of VUSPIO TEG4 R32, measured R_2* signal tended to increase due to the accumulation of the MR contrast agent. The same was observed at 24 h although the increase was less prominent. In contrast, no measurable R_2*change was observed after VUSPIO 0 injection. Because of the absence of plaques in the aorta, no accurate segmentation of pixels corresponding to an atheroma plaque was possible before and after the injection of VUSPIO TEG4 R32 in control C57BL6 mice (Figure S8 in Supporting Information). Figure 5, *B* presents the resulting mean R_2* values of at least six slices from six independent ApoE$^{-/-}$ mice. A significant increase of R_2* was confirmed at 20 min post injection (P = 0.0001). This difference was also found significant compared to the mean R_2* measured consecutively to the injection of VUSPIO 0. No significant differences were found 24 h after injection (P = 0.068). Nevertheless, this P value, although above the significance threshold, was relatively small compared to the corresponding p value measured with the VUSPIO 0 (P = 0.95), accounting for a slight persistence of the VUSPIO TEG4 within the plaque at 24 h post injection.

Fluorescence biodistribution studies showed a clear advan tage in the uptake of multivalent targeted VUSPIOs in the aorta compared to untargeted ones. Figure 5, *C D* shows a typical fluorescence distribution after 24 h in a multivalent VUSPIO TEG4 injected ApoE$^{-/-}$ mice. The most intense signals were displayed by the liver, kidneys, and urine, which are relevant with nanoparticles elimination pathways. All particles had been cleared from the blood and did not distribute into the lungs or muscles. Interestingly, the extremely strong signal in the liver creates a halo that impedes correct signal detection from the other organs; therefore, the biodistribution image had to be acquired in the absence of the liver. Figure 5, *D* shows a comparison of the fluorescence signal of aortas in VUSPIO TEG4 injected and VUSPIO 0 injected mice. Note that the scale of the image was adjusted to emphasize the fluorescence found located all along the aorta for the VUSPIO TEG4. Using the same scale failed to demonstrate fluorescence along the aorta of a VUSPIO 0 injected mouse. Statistical results are summarized in Table 1. No significant biodistribution difference was observed between the injection of targeted VUSPIO and VUSPIO 0 except for the VUSPIO TEG4 injected aorta, which showed a relative fluores cence signal twice as intense as the signal detected in the aorta injected with VUSPIO 0.

Table 1
Biodistribution of the relative fluorescence signals measured 24 h post injection.

Organ	Liver	Kidney	Heart	Spleen	Aorta
VUSPIO TEG4	Sat. S.	100 ± 8.9%	50.4 ± 18.7%	30.3 ± 7.7%	16.7 ± 5.0%
VUSPIO 0	Sat. S.	100 ± 7.8%	46.1 ± 23.6%	29.9 ± 5.85%	7.8 ± 3.4%
P value (Student's *t* test)	N/A	0.86	0.81	0.94	0.04

Discussion

In a previous study, we showed that TEG4, a human antibody selected by phage display against platelet integrin αIIbβ3, and produced under a full rIgG4 format, was able to recognize atheroma plaques in mouse, rabbit and human alike.[11] Here we used a smaller format, TEG4 2c scFv, engineered to harbor terminal cysteines which allowed for oriented and site specific grafting to the terminal maleimide functions borne by VUSPIO nanoparticles.[19] Surface plasmon resonance experiments showed that this newly engineered format was able to bind to its target, the purified integrin αIIbβ3, both unconjugated and after conjugation to nanoparticles, justifying the interest of this oriented grafting. It was further proven by immunofluorescence experiments that this format maintained its reactivity to atheroma lesions as it was shown to label the same structures as a commercial anti CD41 antibody (see Supporting Information), both before and after conjugation.

In this previous study, we also described the conjugation of TEG4, as a full rIgG4 format, to VUSPIO nanoparticles.[11] Although this particle, called VUSPIO TEG4 rIgG4, was able to recognize platelets and atheroma *in vitro*, *in vivo* binding could not be demonstrated. A possible reason for this was that, with an average of only one antibody per VUSPIO, the avidity of the particle was not sufficient to ensure persistent homing *in vivo*. Therefore, in the present study, the TEG4 2c scFv format was chosen in order to minimize the steric hindrance of the targeting agent and consequently to allow for increasing the conjugation ratio. Here, we achieved a maximum ratio of 16 scFv per VUSPIO and we demonstrated the positive influence of this multifunctionalization on both the contrast agent avidity on integrin αIIbβ3 and the atheroma plaque recognition *in vitro*. Indeed, free TEG4 2c scFv were found to rapidly dissociate

from the αIIbβ3 functionalized surface in SPR. In contrast, multivalent VUSPIO TEG4 hardly dissociated from the target, suggesting near irreversible interactions on immobilized αIIbβ3. The sensorgrams obtained when the multivalent VUSPIO TEG4 batches were injected sequentially at increasing concentrations could not be fitted with a 1:1 model of interaction, highlighting a complex binding reaction that likely involves avidity effects and a pseudo rolling mechanism on the sensor chip. Note that the latter was coated with around 2000 RU (2 ng/mm^2) of αIIbβ3 integrin, a protein density chosen to reflect endogenous αIIbβ3 receptor densities at the surface of activated platelets, and thus to reflect the *in vivo* interaction of VUSPIO TEG4 encountering activated platelets in atheroma. Multivalent interactions (multiple ligands to multiple receptors) between nanoparticles and their targets are indeed a well known mechanism adopted by living organisms to facilitate the attachment of pathogens to host cells or immune cells to vascular endothelium.[26,27] In our case, multivalence should benefit to *in vivo* targeting with an improvement of the retention time at the lesion site.

Subsequently, the observed *in vitro* behavior of VUSPIO TEG4 was confirmed by immunohistochemistry experiments. We showed an improvement in atheroma plaques labeling when increasing the ratio between TEG4 2c scFv and VUSPIO nanoparticles (Supporting Information).

Homing of VUSPIO TEG4 to atherosclerotic lesions was then demonstrated by *in situ* targeting assessment in ApoE$^{-/-}$ mice. Taking advantage of the dual imaging modality offered by the VUSPIO platform, an MRI protocol combined with NIRF imaging was established to permit successive quantifications of: (1) the MR signal modulation (R_2* map) mediated by the iron oxide nanoparticles and (2) the fluorescence signal arising from the near infrared fluorochromes appended to the VUSPIO. A specific contrast agent driven R_2* enhancement of the atheroma plaques was detected by MRI at 7 T, confirmed by a matching NIRF signal distribution and consistent with the observed atherosclerotic lesions pattern.

Finally, the potential of VUSPIO TEG4 as an atheroma targeting contrast agent was evaluated *in vivo*. In this study, *in vivo* axial MR images were acquired in the abdominal region for two main reasons. First, it allowed us to minimize the MR motion artifacts that could corrupt the R_2* measurements, *e.g.* the heart beating. Second, at this level, the aorta is surrounded by the paraspinal muscles and by the liver, which limits the presence of constant magnetic field variation (ΔB_0), usually produced by air filled organs such as the lungs or the stomach, responsible for an artificial increase of R_2*. MR imaging highlighted a statistically significant R_2* enhancement in the plaque 20 min after injection ($P = 0.0001$), which persisted 24 h after injection, although with a P value of 0.059. In addition, biodistribution studies performed in *in vivo* injected animals tended to prove a real benefit from VUSPIO multivalent functionalization on plaque recognition 24 h after injection.

The property of the contrast agents to accumulate into the lesions during a given period of time is still a matter of debate: in 2008, a study by Briley Saebo et al[22] hypothesized that, in order to enter the plaque, rigid objects like USPIO (ultrasmall paramagnetic iron oxide nanoparticles) had to be small enough to fit through the vascular fenestrae of the impaired endothelium. The estimated maximum size was reported to be this of native lipoproteins, up to 25 nm. Later, lipid coated USPIO (LUSPIO), inferior to 20 nm in size, and functionalized with antibodies targeting oxidation specific epitopes, showed a superior accumulation in plaque macrophages than their non targeted counterpart.[25] In addition, they showed a superior MR signal attenuation than either targeted or untargeted lipid coated superparamagnetic iron oxide, theoretically more potent but displaying a size between 35 and 40 nm, which was hypothesized to impair their accumulation into the plaque. On the other hand, gadolinium (Gd) loaded micelles, although superior to 100 nm in size, were still able to squeeze through assumed 25 nm diameter pores and be taken up by macrophages.[28,29] Hence, the size but also the flexibility of nanoparticles are to be considered when looking at their ability to enter the plaque and it is not clear whether 25 nm is a clear cut limit for fenestration in the mouse model. Accordingly, the VUSPIO hydrodynamic size of approximately 90 nm before functionalization may constitute a limitation to their entrance through the vascular fenestrae. Interestingly, the diameter distribution of VUSPIO follows a Gaussian model, meaning that a fraction of the injected particles may be small enough to enter the plaque. In addition, in the case of our study with TEG4 2c scFv targeting activated platelets, the particle, if not internalized, could bind to the arterial wall of atheroma lesions. However, it is likely that the stringency of arterial blood flow disturbs the particles binding, decreasing the number of attached VUSPIO TEG4 nanoparticles at the lesion site over time. This could explain the decrease in contrast enhancement after 24 h by MRI. Is it noteworthy that, in the perspective of the clinical application of the object, an imaging sequence 20 min after injection could reveal more manageable than 24 h later. Nevertheless, as a perspective to overcome retention time issues, formulation improvements should work at increasing the power of PEGylation[30] and decreasing the mean size of the nanoparticles in order to exhibit longer circulation times and favor entering within the plaque, respectively.

Associated content

Supporting information available

Details of the TEG4 2c scFv production are provided. Immunofluorescence on mouse, rabbit and human tissue, as well as co staining, is then presented. The full protocol for Site specific multivalent grafting onto VUSPIO nanoparticles and Conjugation ratio measurement is also included, as well as the details for Avidity measurement experiments. Finally, Relaxivity measurements and Data analysis and processing are detailed.

Appendix A. Supplementary data

Supplementary data to this article can be found online at https://doi.org/10.1016/j.nano.2019.102082.

Acknowledgment

This work has benefited from the Vivoptic imaging platform supported by France Life Imaging. More particularly, we would like to thank C. Genevois for her technical support. This work has benefited from the facilities and expertise of the Biophysical and Structural Chemistry plateform (BPCS) at IECB, CNRS UMS3033, Inserm US001, Bordeaux University http://www.iecb.u bordeaux.fr/index.php/fr/plateformestechnologiques. The microscopy was done in the Bordeaux Imaging Center a service unit of the CNRS INSERM and Bordeaux University, member of the national infrastructure France BioImaging supported by the French National Research Agency (ANR 10 INBS 04). The help of Sébastien Marais is acknowledged. We would like to thank the Haut Lévèque Hospital in Pessac, France, for providing the human biological material.

References

1. Benjamin EJ, Blaha MJ, Chiuve SE, *et al.,* Heart disease and stroke statistics 2017 update: a report from the American Heart Association. *Circulation* [Internet]. (2017). Available from: , http://circ.ahajournals.org/content/early/2017/01/25/CIR.0000000000000485.
2. Tsimikas S, Miyanohara A, Hartvigsen K, et al. Human oxidation specific antibodies reduce foam cell formation and atherosclerosis progression. *J Am Coll Cardiol [Internet]* 2011;**58**(16):1715 27 Available from, http://www.ncbi.nlm.nih.gov/pmc/articles/PMC3230644/.
3. Ponnuswamy P, Van Vré EA, Mallat Z, Tedgui A. Humoral and cellular immune responses in atherosclerosis: spotlight on B and T cells. *Vascul Pharmacol* 2012;**56**(5 6):193 203.
4. Ait Oufella H, Taleb S, Mallat Z, Tedgui A. Recent advances on the role of cytokines in atherosclerosis. *Arterioscler Thromb Vasc Biol* 2011;**31**(5):969 79.
5. Cushing SD, Berliner JA, Valente AJ, et al. Minimally modified low density lipoprotein induces monocyte chemotactic protein 1 in human endothelial cells and smooth muscle cells. *Proc Natl Acad Sci U S A* 1990;**87**(13):5134 8.
6. Vora DK, Fang Z T, Liva SM, et al. Induction of P selectin by oxidized lipoproteins separate effects on synthesis and surface expression. *Circ Res [Internet]* 1997;**80**(6):810 8 Available from, http://circres.ahajournals.org/content/80/6/810.
7. Virmani R, Kolodgie FD, Burke AP, Farb A, Schwartz SM. Lessons from sudden coronary death a comprehensive morphological classification scheme for atherosclerotic lesions. *Arterioscler Thromb Vasc Biol [Internet]* 2000;**20**(5):1262 75 Available from, http://atvb.ahajournals.org/content/20/5/1262.
8. Insull Jr. W. The pathology of atherosclerosis: plaque development and plaque responses to medical treatment. Am J Med [Internet]. 122(1, Supplement), S3 S14 (2009). Available from: , http://www.sciencedirect.com/science/article/pii/S0002934308010176.
9. Nording HM, Seizer P, Langer HF. Platelets in inflammation and atherogenesis. *Front Immunol* 2015;**6** Internet. Available from, http://www.ncbi.nlm.nih.gov/pmc/articles/PMC4351644/.
10. Badrnya S, Schrottmaier WC, Kral JB, et al. Platelets mediate oxidized low density lipoprotein induced monocyte extravasation and foam cell formation. *Arterioscler Thromb Vasc Biol* 2014;**34**(3):571 80.
11. Jacobin Valat M J, Laroche Traineau J, Larivière M, et al. Nanoparticles functionalised with an anti platelet human antibody for in vivo detection of atherosclerotic plaque by magnetic resonance imaging. *Nanomedicine Nanotechnol Biol Med [Internet]* 2015;**11**(4):927 37 Available from, http://www.sciencedirect.com/science/article/pii/S154996341500012X.
12. Tarkin JM, Dweck MR, Evans NR, et al. Imaging atherosclerosis. *Circ Res* 2016;**118**(4):750 69 Internet. Available from, http://circres.ahajournals.org/content/118/4/750.
13. Lobatto ME, Calcagno C, Millon A, et al. Atherosclerotic plaque targeting mechanism of long circulating nanoparticles established by multimodal imaging. *ACS Nano* 2015;**9**(2):1837 47.
14. Beldman TJ, Senders ML, Alaarg A, et al. Hyaluronan nanoparticles selectively target plaque associated macrophages and improve plaque stability in atherosclerosis. *ACS Nano* 2017;**11**(6):5785 99.
15. Bruckman MA, Jiang K, Simpson EJ, et al. Dual modal magnetic resonance and fluorescence imaging of atherosclerotic plaques in vivo using VCAM 1 targeted tobacco mosaic virus. *Nano Lett* 2014;**14**(3):1551 8, https://doi.org/10.1021/nl404816m Internet. Available from.
16. Kheirolomoom A, Kim CW, Seo JW, et al. Multifunctional nanoparticles facilitate molecular targeting and miRNA delivery to inhibit atherosclerosis in ApoE / mice. *ACS Nano* 2015;**9**(9):8885 97, https://doi.org/10.1021/acsnano.5b02611 Internet. Available from.
17. Jacobin M J, Laroche Traineau J, Little M, *et al.* Human IgG monoclonal anti alpha(IIb)beta(3) binding fragments derived from immunized donors using phage display. *J. Immunol. Baltim. Md* 1950. 168(4), 2035 2045 (2002).
18. Mornet S, Portier J, Duguet E. A method for synthesis and functionalization of ultrasmall superparamagnetic covalent carriers based on maghemite and dextran. *J Magn Magn Mater [Internet]* 2005;**293**(1):127 34 Available from, http://www.sciencedirect.com/science/article/pii/S030488530500140X.
19. Vallet Courbin A, Larivière M, Hocquellet A, *et al.* A recombinant human anti platelet scFv antibody produced in Pichia pastoris for atheroma targeting. PloS One [Internet]. 12(1), e0170305 (2017). Available from: , http://journals.plos.org/plosone/article?id 10.1371/journal.pone.0170305.
20. Chu B, Ferguson MS, Chen H, et al. MRI features of the disruption prone and the disrupted carotid plaque: a pictorial essay. *JACC Cardiovasc Imaging [Internet]* 2009;**2**(7):883 96 Available from, http://www.ncbi.nlm.nih.gov/pmc/articles/PMC2793180/.
21. Petibon Y, El Fakhri G, Nezafat R, Johnson N, Brady T, Ouyang J. Towards coronary plaque imaging using simultaneous PET MR: a simulation study. *Phys Med Biol* 2014;**59**(5):1203 22, https://doi.org/10.1088/0031 9155/59/5/1203/meta Internet. Available from.
22. Briley Saebo KC, Mani V, Hyafil F, Cornily J C, Fayad ZA. Fractionated feridex and positive contrast: in vivo MR imaging of atherosclerosis. *Magn Reson Med* 2008;**59**(4):721 30, https://doi.org/10.1002/mrm.21541 Internet. Available from.
23. Michalska M, Machtoub L, Manthey HD, et al. Visualization of vascular inflammation in the atherosclerotic mouse by ultrasmall superparamagnetic Iron oxide vascular cell adhesion molecule 1 specific nanoparticles. *Arterioscler Thromb Vasc Biol [Internet]* 2012;**32**(10):2350 7, https://doi.org/10.1161/ATVBAHA.112.255224 Available from.
24. Makowski MR, Forbes SC, Blume U, et al. In vivo assessment of intraplaque and endothelial fibrin in ApoE / mice by molecular MRI. *Atherosclerosis* 2012;**222**(1):43 9 Internet. Available from, http://www.sciencedirect.com/science/article/pii/S0021915012000123.
25. Briley Saebo KC, Cho YS, Shaw PX, et al. Targeted iron oxide particles for in vivo magnetic resonance detection of atherosclerotic lesions with antibodies directed to oxidation specific epitopes. *J Am Coll Cardiol [Internet]* 2011;**57**(3):337 47 Available from, http://www.ncbi.nlm.nih.gov/pmc/articles/PMC3095034/.
26. Lee RT, Lee YC. Affinity enhancement by multivalent lectin carbohydrate interaction. *Glycoconj J* 2000;**17**(7 9):543 51.
27. Mammen M, Choi S K, Whitesides GM. Polyvalent interactions in biological systems: implications for design and use of multivalent ligands and inhibitors. *Angew Chem Int Ed* 1998;**37**(20):2754 94.
28. Briley Saebo KC, Amirbekian V, Mani V, et al. Gadolinium mixed micelles: effect of the amphiphile on in vitro and in vivo efficacy in

apolipoprotein E knockout mouse models of atherosclerosis. *Magn Reson Med* 2006;**56**(6):1336 46, https://doi.org/10.1002/mrm.21094/abstract Internet. Available from.

29. Maiseyeu A, Mihai G, Kampfrath T, et al. Gadolinium containing phosphatidylserine liposomes for molecular imaging of atherosclerosis. *J Lipid Res* 2009;**50**(11):2157 63.
30. Adumeau L, Genevois C, Roudier L, Schatz C, Couillaud F, Mornet S. Impact of surface grafting density of PEG macromolecules on dually fluorescent silica nanoparticles used for the in vivo imaging of subcutaneous tumors. *Biochim. Biophys. Acta BBA - Gen. Subj.* [Internet]. Available from: , http://www.sciencedirect.com/science/article/pii/S0304416517300442.